

The Permeability Characteristics of Dry Fiber Preforms Manufactured using Automated Dry Fiber Placement

R.A. Alia^{*1}, R. Umer², X. Zeng², S. Rao¹, W.J. Cantwell¹

¹Aerospace Research and Innovation Center, Khalifa University of Science and Technology (KUST), Abu Dhabi, UAE., *alia.aziz@kustar.ac.ae

²Centre for Future Materials, University of Southern Queensland, Toowoomba, QLD 4350, Australia.

Keywords: Permeability, Preform, Automated dry fiber placements, Finite elements

ABSTRACT

Automated fiber placement (AFP) preforms are especially attractive for applications in aerospace and marine industries. However, there are various challenges in predicting the performance of the preform that are associated with the complexity of the structure. The work presented here aims towards gaining an understanding of the permeability characterization of dry fiber placement preforms. Initially, a numerical analysis of a simplified dry tape preform model, with the focus on the through-thickness permeability has been undertaken. Geometrical models consisting of the flow channels of the carbon dry tape preform are created and Computational Fluid Dynamics (CFD) simulations are then executed using the commercial code ANSYS/CFX to obtain the predicted permeability characteristics of the preform. An XCT scan conducted on the preform revealed that the gap sizes are irregular throughout the preforms. In the final part of this study, an experimental investigation of the through-thickness permeability is presented. The CFD predictions for the permeability of the preform are compared with the experimental data.

1 INTRODUCTION

Composite materials are now widely used in large and complex structures in the aerospace industry due to their high-strength to weight ratio compared to other conventional materials. Difficulties in manufacturing large complex composite parts drive many companies to develop new methods and techniques to obtain improved part quality. Technologies are developed to produce preforms by fabric draping, fabric stitching or weaving 3D profiles. However, these procedures are labour-intensive, expensive and rely heavily on textile processing capabilities. The robotic automated fiber placement (AFP) technique [1, 2] offers many features and advantages over the traditional fabrication techniques. The AFP technique involves depositing fibers onto a complex mold at a high rate, overcoming any fabric structure variability and variations in local fiber volume fractions, while draping in tight corners. In the lay-up operation used for dry fiber AFP, the tows are either delivered to the head from a creel cabinet, or stored directly on the head [2]. The dry fiber placement process requires the use of a thermoplastic binding agent and a permeable veil between the fibers, the quantity used should be enough to tack to the mold and subsequent layers when heated, whilst retaining the preform shape prior to resin injection.

Permeability characterises the ease with which a fluid can flow through the reinforcement and is primarily a function of the reinforcement architecture and its fiber volume fraction. Woven fabrics, as well as non-crimp fabrics, are dual-scale porous media and generally exhibit different permeabilities in different material directions, i.e. the values of the two in-plane permeabilities, K_{11} and K_{22} , and the through-thickness permeability, K_{33} , are different. Although determining the whole permeability tensor is important, the through-thickness permeability is crucial in controlling the thickness of the cured product. With increasing preform thickness, the influence of through-thickness permeability on RTM processing of composites becomes increasingly significant [3]. When resin injection is in the through-thickness direction, K_{33} becomes the dominant deciding parameter.

Clearly, a detailed study is required to adjust the tow gap to achieve a superior flow behavior and mechanical properties [1]. Belhaj et al. [4] employed three different preform configurations, by adjusting the tow gap, to study the permeability and compaction behavior of preforms. They concluded that different configurations affected the resulting mechanical properties and that the creation of open channels, to enhance the flow propagation during manufacture, did not increase the preform permeability to any significant degree. Recent research on the out-of-plane permeability of preforms has focused on the experimental analysis by varying several parameters in order to enhance the permeability [5, 6] however little research has considered a computation modelling approach for the preform for a faster and reliable prediction. This study starts with a numerical analysis of a simplified preform model, with the focus on the through-thickness permeability direction, K_{33} . In the next part, a detailed structure analysis and the permeability of the preform will be experimentally obtained and compared to the finite element results.

2 MATERIALS

The preforms were manufactured using the automated fiber placement (AFP) manufacturing technique and supplied by Cytec Ltd. (Wrexham). Here, a Coriolis AFP machine with a KUKA robot and a 6 kW laser mounted on the end-effector, was used to place the fibers on a flat mold. The heat generated by the laser was sufficient to activate a thermoplastic binder that ensured bonding of adjacent tows. The panels were manufactured after adjusting the tow gap to facilitate resin flow. 6.35 mm and 12.7 mm tape preforms, with tow gaps of 0.2 mm, were investigated. The preform consists of 24 layers with a stacking sequence of $[+45/0/-45/90]_{3s}$, giving an overall thickness of 5.15 mm. For the reinforcement, unidirectional Tenax IMS65 carbon fibers with a filament diameter of 5 μm were used. The material data specifications are listed in Table 1.

Property	AFP tape
Fiber type	Tenax IMS65 Carbon fiber
Fiber density [g/cm^3]	1.78
Fiber diameter [μm]	5
Fiber tensile strength [MPa]	6000
Fiber tensile modulus [GPa]	290
Fiber elongation at break [%]	1.9
Tape thickness [mm]	0.2
Number of layers	24
Preform thickness [mm]	5.15
Gap width and height [mm]	0.2
Stacking sequence	$[+45/0/-45/90]_{3s}$

Table 1: Material data for the 6.35 mm and 12.7 mm AFP tape preforms.

3 MODEL DEVELOPMENT

3D geometrical models of the tape preform were created in the TexGen modeller using a graphical user interface (GUI). The dry tape geometries were modelled as per the manufacturer's design with tape thickness, gap width and height of 0.2 mm. For the dry tape preform studied here, the tapes were assumed to be impervious to flow as the permeability, which can be approximated by Gebart's model [7]. Hence, steady-state flow through the channels was modelled, given that the fluid will travel more rapidly through the gaps between the tapes. This assumption greatly reduces the computational cost of the flow simulation. Figure 1(a) shows a dry tape preform model, created by stacking layers of unidirectional tape in a $[+45/0/-45/90]_{3s}$ stacking sequence. In order to discretise the preform into computational mesh, appropriate number and type of elements were defined in the x, y and z directions.

Computational fluid dynamics (CFD) simulations were carried out using the commercial code ANSYS/CFX for the permeability analysis of the generated matrix mesh imported from ANSYS/finite element modeller. In the CFX-Pre processor, the boundary conditions are defined. Figure 1 shows the preform flow channels and the boundary conditions for the dry tape used in the ANSYS model for through-thickness permeability predictions. The numerical study conducts a laminar flow simulation, with a pressure gradient applied in the flow direction, with a pressure length of 4.8 mm, i.e. the thickness of the preform. Non-slip wall boundary conditions were specified at the four side surfaces of the fluid domain, as well as between the tapes and the fluid interfaces for the through-thickness flow simulation.

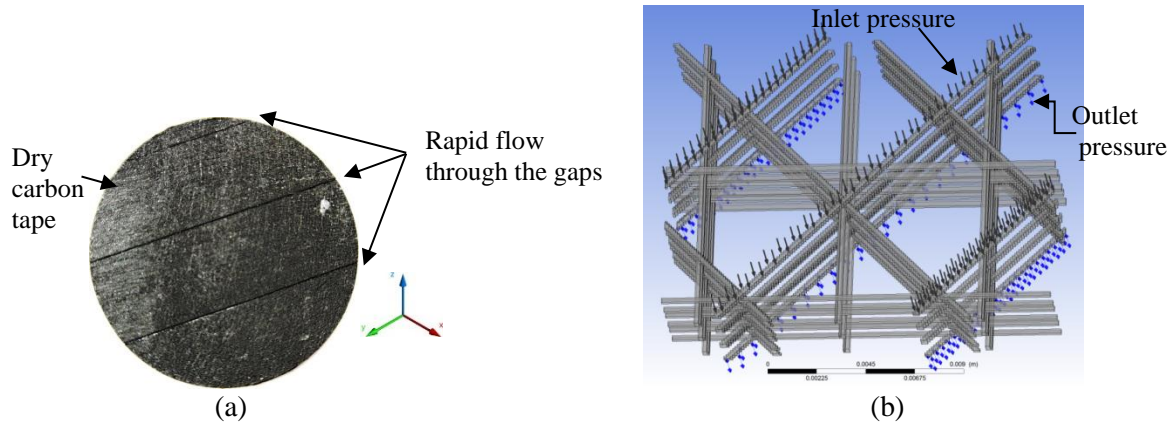


Figure 1: A carbon dry preform (a) flow channels and (b) the boundary conditions used in the model.

Once the simulation parameters were defined in the CFX-Pre processor, the CFX-Solver was used to run and solve all of the flow field variables for flow simulation based on discretisation of Navier-Stokes continuity and momentum equations [8]. ANSYS CFD-Post is used for postprocessing the simulation results and to obtain the necessary information for permeability calculations. During the post-processing stage, the flow paths are visualised and volume averaged mass flow-rate is obtained. With the applied pressure gradient and known geometry, the permeability through the gaps between the tapes is calculated according to Darcy's law given in Equation 1 as follows [7]:

$$\frac{m'}{\rho} = \frac{kA}{\mu} \frac{P_1 - P_2}{L} \quad (1)$$

where k is the permeability through the gaps, A is the cross-section area, m' is the mass flow rate, μ is the liquid viscosity, ρ is the liquid density, L is the preform thickness, and $P_1 - P_2$ is the pressure drop. To obtain a reasonable balance between computation time and accuracy, the sensitivity of the CFX calculations to the mesh size was assessed, based on convergence of the predicted through-thickness permeability of the AFP tape. The CFD results for the through-thickness permeability are compared to the experimental data.

4 EXPERIMENTAL

X-ray computerized tomographic (XCT) images were obtained using a GE Phoenix Nanotom device to study the microstructure of the preform, specifically the gaps between the tapes. A series of 2D radial slices of X-ray absorption maps were captured by rotating the sample through 360° in 1500 steps. This compilation of data is then used to reconstruct the tomographic image. In obtaining the XCT images, no pre- or post-filters were used for the sample scans. The preform sample size used in this analysis was 40 mm in diameter. The XCT experimental set-up is presented in Figure 2(a).

A compaction fixture was installed in the XCT machine with a load cell capacity of 5 kN. The preforms were placed between the two platens and compaction load equivalent to full vacuum pressure was applied. Both the 6.35 and 12.7 mm wide tape preforms were compressed and scanned at a thickness of 4.8 mm. The commercial packages, VGStudio Max and GeoDict, were used for data

processing, evaluation and porosity analysis. A bimodal threshold was applied on the voxel intensity histogram to segment the pores and the preform [9, 10]. Following the microstructural analysis, the through-thickness permeability was measured using an existing saturated unidirectional flow measurement device, as shown in Figure 2(b). The device was housed within a 300 kN MTS testing frame, allowing for accurate control of sample thickness, and the potential for simultaneous compressibility and permeability measurements. In the cylindrical fixture, the flow direction is from the bottom inlet to the top flow outlet, passing through plates with holes. This allows through-thickness parallel flow of the liquid, perpendicular to the preform. In this study, permeability measurements were made at one fiber volume fraction, corresponding to vacuum pressure for each sample. A series of increasing pressure drops were applied across the sample, and the resulting fluid flow rates measured. The flow rate was defined by measuring the variation of the mass of the pressure pot with time.

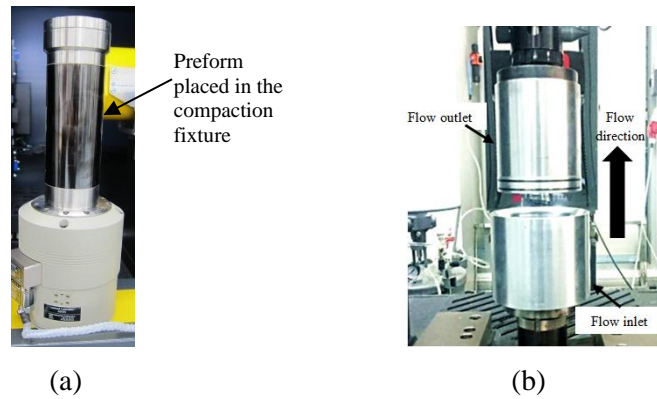


Figure 2: Experimental set-up of (a) the XCT fixture and (b) the cylindrical through thickness flow fixture.

5 RESULTS AND DISCUSSIONS

The flow velocity values were obtained from the CFX post-processor and the permeability was calculated by applying Darcy's law. From the mesh sensitivity analysis, it was found that an element size of 0.05 mm was deemed to be appropriate, since it produces sufficiently accurate results in a short CPU time. Table 2 presents the predicted FE results for the through-thickness permeability for the 6.35 and 12.70 mm AFP dry tapes. The percentage porosity in the 3D model is based on the ratio of the volume of the gaps to the total volume of the domain. By applying the manufacturer's data dimensions in the FE models, the porosities for 6.35 and 12.7 mm samples were approximately 3.1% and 1.5% respectively. The permeability in the through-thickness direction obtained from CFX analyses of the 6.35 mm and 12.7 mm samples were 3.87×10^{-13} and $3.65 \times 10^{-14} \text{ m}^2$, respectively. Clearly, the permeability for the 12.70 mm tape is approximately 90% lower than the 6.35 mm tape. A higher flow channel density can be observed in the 6.35 mm tape compared to 12.7 mm preform model. This visual observation suggests that the permeability is much higher in the 6.35 mm preform, which agrees with the FE permeability results.

Sample	Porosity [%]			Permeability [m^2]		
	XCT	FE	Ratio XCT-FE	Experiment	FE	Ratio Exp-FE
6.35 mm	1.5	3.1	0.5	8.31×10^{-14}	3.87×10^{-13}	0.2
12.7 mm	3.5	1.5	2.3	1.85×10^{-13}	3.65×10^{-14}	5.1

Table 2: Porosity and permeability values for the preforms.

A visual inspection of on the preform samples revealed that there were slight irregularities in the gap sizes. Therefore, an XCT scan was a conducted on the preforms to study the pore size distribution. Before scanning the samples, the preforms were compressed inside the XCT scanner to a 58% volume fraction. The reconstructed images of the preforms taken from XCT were analyzed using the VGStudio MAX software. Figure 3(a) represents a typical 3D XCT scan image with the entire pores of the preform shown. This image was then transferred to Geodict software, where the software segments the tapes as a solid section and the gaps as pores. A closer inspection of the Figure 3(b) image revealed that some gaps are noticeably wider than others. From the pore distribution analysis, it was found that the measured porosities of 6.35 and 12.7 mm preforms were approximately 1.5% and 3.5% respectively.

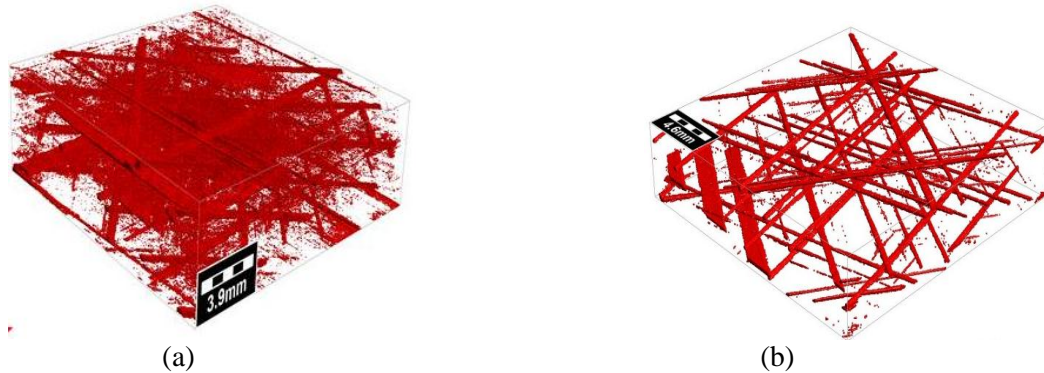


Figure 3 Geodict analysis showing the distribution of pores.

The experimental results for the through-thickness permeability of the preforms are summarised in Table 2. The permeability of the 12.7 mm tape is approximately twice that of the 6.35 mm tape, with the former being $1.85 \times 10^{-13} \text{ m}^2$ and the latter $8.31 \times 10^{-14} \text{ m}^2$. The permeabilities derived from FE simulations are compared with experimental data. An examination of the table indicates that the FE model of the 6.35 mm preform overestimates the average experimental data by over 4.7 times. This relatively large difference is associated with the perfect geometry that was employed in the FE models, where the actual dimensions of the preform samples were not considered. An examination of the 6.35 mm preform in the XCT scan revealed that the porosity in this sample was approximately 2.1 times lower than that in the FE models. In contrast, Table 2 shows that the FE prediction for the 12.7 mm tape underestimates the experimental value of permeability by approximately 5.1 times.

In theory, the geometrical dimensions of the gaps over the entire sample should be measured in order to achieve a more accurate prediction of the permeability of these preforms. Nonetheless, this is likely to be unfeasible, given the large number of gaps that are present in a preform that is based on a complex fiber stacking sequence. The FE analysis results can be used for preliminary predictions by correcting the numerical data from the parametric analyses by the factors outlined above.

6 CONCLUSIONS

The work that is presented here is encouraging for the numerical permeability prediction of the preform. Agreement between the models consisting of the flow channels of preform and the experimental results is reasonable in obtaining the predicted permeability characteristics. A detailed XCT scan performed on the sample shows that the gap sizes are irregular throughout the preforms. Hence, the numerical data from the parametric analyses need to be corrected by multiplying these values by certain factors. In a future step, it would be interesting to convert the XCT images from pore distribution analysis into a 3D model to generate a more realistic geometry model that will result in greater accuracy in the permeability predictions.

ACKNOWLEDGEMENTS

The authors would like to thank Mr. Pradeep George and Mr. Prabu Raja at Khalifa University for their assistance in conducting the experiments. This research was performed as part of the Aerospace Research & Innovation Center (ARIC) program which is jointly-funded by Mubadala Aerospace and Khalifa University.

REFERENCES

- [1] K. Croft, L. Lessard, D. Pasini, M. Hojjati, J. Chen, and A. Yousefpour, Experimental study of the effect of automated fiber placement induced defects on performance of composite laminates, *Composites Part A: Applied Science and Manufacturing*, 42, 2011, pp484–491.
- [2] D. H. J. A. Lukaszewicz, C. Ward, and K. D. Potter, The engineering aspects of automated prepreg layup: History, present and future, *Composites Part B: Engineering*, 43, 2012, pp997–1009.
- [3] X. Xiao, A. Endruweit, X. Zeng, J. Hu, and A. Long, Through-thickness permeability study of orthogonal and angle-interlock woven fabrics, *Journal of Materials Science*, 50, 2015, pp1257–1266.
- [4] M. Belhaj *et al.*, Dry fiber automated placement of carbon fibrous preforms, *Composites Part B: Engineering*, 50, 2013, pp107–111.
- [5] R. Graupner, Material efficient Dry Fiber Placement preforming process with adapted lay-up strategies for off-plane impregnation, in 5th anniversary of LCC Symposium, Munich.
- [6] O. Rimmel, D. Becker, and P. Mitschang, Maximizing the out-of-plane-permeability of preforms manufactured by dry fiber placement, *Advanced Manufacturing: Polymer & Composites Science*, 2, 2016, pp93–102.
- [7] B. R. Gebart, Permeability of Unidirectional Reinforcements for RTM, *Journal of Composite Materials*, 26, 1992, pp1100–1133.
- [8] B. Verleye *et al.*, Permeability of textile reinforcements: Simulation, influence of shear and validation, *Composites Science and Technology*, 68, 2008, pp2804–2810.
- [9] G. Chinga-Carrasco, O. Solheim, M. Lenes, and Å. Larsen, A method for estimating the fibre length in fibre-PLA composites, *Journal of Microscopy*, 250, 2013, pp15–20.
- [10] E. N. Landis and D. T. Keane, X-ray microtomography, *Materials Characterization*, 61, 2010, pp1305–1316.